

**THE ORIGIN OF GILSONITE VEIN DEPOSITS  
IN THE UINTA BASIN, UTAH**

*by*

*B. Monson and J. Parnell  
The Queen's University of Belfast  
Belfast, BT7 1NN, Northern Ireland*

**CONTRACT REPORT 92-4  
UTAH GEOLOGICAL SURVEY**

**a division of**

**UTAH DEPARTMENT OF NATURAL RESOURCES**

**MARCH 1992**

**THE PUBLICATION OF THIS PAPER  
IS MADE POSSIBLE WITH MINERAL LEASE FUNDS**

**A primary mission of the UGS is to provide geologic information of Utah through publications. This Contract Report represents material that has not undergone policy, technical, or editorial review required for other UGS publications. It provides information that, in part, may be interpretive or incomplete and readers are to exercise some degree of caution in the use of the data. The UGS makes no warranty of the accuracy of the information contained in this publication.**

## ABSTRACT

A series of fractures are infilled with veins of the solid bitumen gilsonite in the eastern Uinta Basin. A proposed model for formation involves two distinct stages. Firstly hydrofracturing was caused by elevated pore pressures, probably initiated in the Green River Formation. Secondly the fractures were injected by liquid hydrocarbon, sourced from the Green River Formation, which subsequently solidified to form veins.

## INTRODUCTION

Veins of solid hydrocarbon (bitumen) containing millions of tonnes of hydrocarbon ore occur in several parts of the world. They have been the object of sizeable mining industries in South America, North America and Asia. The hydrocarbon deposits have been given a variety of mineral names (albertite, gilsonite, grahamite etc.) which reflect different stages of organic maturity. Numerous elongate vertical fractures infilled with the solid hydrocarbon gilsonite are exposed in the east of the Tertiary Uinta Basin, Utah (Fig. 1). The largest gilsonite vein may be in excess of 20 km in length; the maximum recorded vein width is 6m. The veins cut portions of the Paleocene and Eocene Wasatch, Green River and Uinta formations and Eocene and Oligocene Duchesne River Formation. These formations are predominantly fluvial and lacustrine, texturally immature sandstones with interbedded siltstones and mudstones, the exception being the Green River Formation, which includes a sequence of kerogen-rich oil shales (Fig. 2).

Gilsonite has been extensively mined since the end of the last century, and at present the veins are being worked by three companies (American Gilsonite, Zeigler Corp. and Lekas Mining). The gilsonite is shipped world-wide and has uses in the production of inks and sealing mastics and has been employed in some types of nuclear reactors as a component of the control rods. We report here the results of a study of the origin of the Uinta Basin gilsonite veins.

The aims of this project were to determine the mechanism of formation of the gilsonite veins. Field observations, thin section, reflectance, fluid inclusion, scanning electron microscopy and electron-microprobe techniques were used to provide new information on the veins. These were combined with hydrocarbon generation modelling techniques and linked with an analysis of the diagenesis of the host sandstones. Previous research has relied predominantly on field observation (Eldridge 1896, Pruitt 1961, and

others) or organic geochemistry (Hunt 1963) and although the source of the gilsonite is generally accepted as being the Eocene part of the Green River Formation there has been little agreement as to the mechanisms of vein formation.

## TECTONIC SETTING

The Uinta Basin probably formed during the late Cretaceous-early Tertiary Laramide orogeny. The effects of orogenic activity on the rocks of the eastern Uinta Basin must have been relatively minor since the rocks in the study area are relatively undeformed and almost flat-lying. Subsequent doming of the Umcomphagre uplift, to the south, may also have occurred, causing slight doming seen in the surrounding rocks. This may have some influence on the formation of the veins (see below).

## STRUCTURE

Gilsonite veins occur in relatively undeformed gently dipping sedimentary rocks, on the southern limb of the Uinta Basin. Apart from the bounding faults of the basin, which lie over 60km to the north of the veins, only one major lineament is evident, the Duchesne fault zone, an east-west striking fault which has a normal displacement. This fault zone probably pre-dates vein formation as traces of gilsonite are found on fault surfaces close to vein intersections (Crawford 1949). A number of major fault systems may underlie the area, including the Gar Meas (Stone, 1977) and these faults may have affected the development of the veins. However the importance of such fault systems on the formation of the veins is difficult to estimate.

The veins are vertical to sub-vertical and are orientated sub-parallel with each other in a predominantly WNW-ESE trend. This trend deflects towards a NW-SE orientation in the northwest of the area of vein outcrop (Fig. 3)

## OBSERVATIONS

### Gilsonite Vein and Wall Rock Relationships

Veins typically appear as planar, vertical-walled structures where they cut through sandstones. However the veins become irregular and break up into an anastomosing network of veinlets where they pass through siltstones and mudstones. The veins are generally straight in plan view.

There are a number of features which modify the generally simple structure seen in the veins cutting the sandstones.

i) Steps are commonly observed in the vein margins, in both horizontal and vertical orientations. Such steps generally are less than the width of the vein (Fig. 4). Apparent displacement was generally sinistral where observed in the horizontal plane.

ii) Small offshoots of gilsonite are observed emanating from the vein, running parallel with the vein and isolating large slabs of country rock which are connected to the wall at the offshoot termination (Fig. 4).

iii) Where the vein passes through finely laminated horizons small offshoots may inject along bedding, forming veinlets normal to the main vein (Fig. 4).

iv) A number of veins exhibit zones of brecciation. These are limited in extent, occupying only a few cubic metres, and are associated with deviations in the trend of the vein. The breccia is gilsonite-supported and gilsonite can be seen cross-cutting individual clasts. The wall rock in the areas of breccia is commonly highly veined by gilsonite which seems to have been injected into small cracks. Authigenic quartz crystals occur on individual clasts of the breccia (Fig. 5).

v) Rock debris accumulated above horizontal steps in the vein. In some cases the rock can be matched with the vein wallrock. Debris did not accumulate beneath the steps.

vi) Impregnation of wallrock sandstones by the gilsonite occurs along the margin of a number of veins. In the most highly impregnated sandstones, the sand grains are free-floating within the gilsonite. Commonly, a tar-like substance can be observed seeping from the vein walls where the gilsonite had been mined out. These features were not common to all the veins, and subsequent petrographic studies show that the

lithology and diagenesis of the host sandstones are the main controlling factors in their development.

vii) A series of parallel joints may be observed up to 10 m on either side of a vein. The intensity of these joints seems to decrease away from the vein. These joints often exhibit plume structures and/or mineralization, features not common on the vein walls, and were rarely seen to contain gilsonite. Slip striae were not recorded on these joints or on the vein walls. Mineral precipitates on the joints include iron oxide, gypsum, calcite and barite. Two joints parallel to the gilsonite vein at Black Dragon, in the south east of the area, were observed to have gilsonite-impregnated sandstones in a zone up to 50 cm on either side, but without a central gilsonite filling. The gilsonite vein at the former mine at this locality this locality also exhibits a surrounding zone of sandstone impregnation.

#### **Petrography and Diagenesis of Sandstone Host Rocks**

A total of 36 vein wallrock samples were examined using thin section and SEM techniques to determine their petrography and diagenetic sequence. This data is summarised in a diagenetic sequence for these rocks (Fig. 6)

##### **1) Detrital Minerals**

Detrital quartz grains are predominantly monocrystalline, with bands of "dusty" inclusions common. The grains appear sub-angular to sub-rounded where the original shape is not masked by overgrowths. Quartz may contribute up to 55% of the detrital component of these rocks.

Potassic feldspars such as orthoclase and microcline are the predominant feldspar component of the sandstones, with appreciable amounts of plagioclase also present. The feldspars exhibit varying degrees of alteration to clays. Feldspars can form in excess of 30% of the detrital grains, 17% being an average proportion.

Lithic fragments are common constituents, commonly making up 25% of the rock. Volcaniclastics and mudstone clasts are the most common varieties with chert and chalcedony fragments also present. The volcaniclastic fragments are commonly

heavily altered to clays with the quartz or feldspar components remaining resistant to alteration. The clasts have undergone varying degrees of ductile deformation as a result of compaction.

Micas, both fresh muscovite and altered biotite, are present in some samples. The micas are commonly deformed around other detrital grains and exhibit splitting or fanning as a result of the deformation.

## 2) Authigenic mineralogy

Varying amounts of authigenic quartz overgrowths can be distinguished due to the presence of dust rims and euhedral crystal terminations. Quartz cementation seems to have been early since specimens with well developed interlocking quartz overgrowths exhibit lesser degrees of compaction. The overgrowths are also commonly replaced by a later calcite cement where calcite is present.

Calcite is only present in some of the samples but its absence from other specimens may be the result of a later phase of dissolution. The calcite appears as pore-filling sparry crystals, commonly partly replacing detrital grains and quartz overgrowths. The presence of calcite in some specimens has arrested the compaction process, indicating that this is a relatively early cement. An albite cement is also present in some specimens but subsequent dissolution has reduced this to a patchy cement. Dolomite and iron carbonates were not recorded from the specimens analysed.

Evidence for a phase of mineral dissolution is present, including oversized pores, corroded quartz grains lacking calcite cement and remnants of calcite, feldspars and lithic fragments within larger pores. This dissolution occurred before a phase of clay mineral precipitation. Analcime occurs in varying amounts as a patchy pore-filling cement, which exhibits euhedral terminations in secondary pores.

The clay mineral phase is predominantly chlorite, with well-developed rosettes of chlorite occurring as grain-coating and pore-filling cements. Chlorite also replaces lithic fragments. However the typical chlorite morphology is not well-developed where formed on corroded grains.

A coating of iron oxides, and in some places gypsum or calcite, was precipitated on fracture walls. The gypsum may represent an early fracture-filling phase or a much later precipitate at the host-rock - vein boundary. This fracture coating is not persistent in the host sandstones. A phase of gilsonite injection is recorded, where the porosity is well developed, with all available porosity in the wallrock sandstones being infilled with gilsonite. The gilsonite appears as an amber to brown-coloured material in thin section. Delicate structures within the chlorite are preserved where the gilsonite is present: the gilsonite envelopes individual blades of chlorite. The presence of a chlorite cement severely restricted the permeability of the host sandstones and gilsonite-impregnated sandstones only occur within the host sandstones a few metres outward from the vein, and are generally absent beyond 30cm. Small amounts of authigenic quartz and barite may be observed "floating" within the gilsonite in the veins.

The paragenetic sequence (Fig. 6) indicates that gilsonite impregnation of the sandstone wallrocks occurred relatively late in the diagenetic history. It is notable, therefore, that at the margins of some veins, gilsonite impregnates the sandstone so effectively that the sand grains appear to float in the gilsonite cement. Furthermore, numerous isolated sand grains may be suspended within the gilsonite vein proper (Fig. 7). The floating and suspended grains were originally part of the cemented sandstone: they exhibit quartz overgrowths (Fig. 8) and evidence for breakage from adjacent grains. It is conceivable that the overgrowths developed after isolation within the gilsonite, as authigenic crystals are recorded from nearby wurtzilite veins (see below). However the size of the overgrowths is identical to that of those in the intact sandstone and it can be assumed that the grains were derived complete with cementing overgrowths from the wallrock. Where veinlets of gilsonite penetrate the wallrock, veins can be seen in various stages of detachment into the gilsonite (Fig. 9). Patches of sandstone well-cemented by albite are relatively weakly impregnated by gilsonite: these are remnants of a formerly more extensive cement which was leached pre-gilsonite impregnation. The relationships

between the sand grains and the gilsonite suggest that the grains were detached from their parent rock, with considerable force, but with a fluid of high enough viscosity to hold the grains in suspension. Many veins contain fragments of mudrock wallrocks. These clasts frequently exhibit fracturing, displacement across the fractures (Fig. 10), and infilling of the fractures by gilsonite, which may also be evidence for vigorous injection of the gilsonite.

Subsequent to the solidification of the gilsonite, further dissolution of calcite and analcime produced a second phase of secondary porosity, and a general reddening of the rocks is also observed. These features are thought to reflect late stage telodiagenetic events.

Examination of the Green River Formation hydrocarbon source rock using backscattered electron microscopy yields some evidence for migration of bitumen through microfractures. Figure 11 shows a veinlet of bitumen cross-cutting the lamination, in a sample collected from the base of the Tabor Vein.

The bitumen in the vicinity of the source rock contains authigenic carbonate crystals, which is not surprising as the Green River Formation oil shales are petrographically dolomitic limestones. Bitumen on bedding planes in the oil shales includes dolomite crystals (Fig. 12), and vertical bitumen veinlets which cross-cut the Green River Formation at the base of the Tabor Vein contain hollow spheres and microveinlets of calcite (Fig. 13). The cracks and bubbles in the gilsonite probably represent shrinkage during solidification.

### Discussion of Diagenesis

The diagenetic sequence seen in the host rocks is similar to that recorded by Pitman and others (1982) for hydrocarbon reservoir rocks of the Uinta Basin. The succession exhibits a sequence progressing from the precipitation of framework-stabilising cements which reduced the effects of compaction, progressing to a phase of dissolution of both cements and detrital grains resulting in the formation of secondary porosity. The secondary porosity is in turn partly infilled by chlorite. Small amounts of analcime and a

subsequent phase of hydrocarbon migration associated with the vein-formation event infill the remaining porosity.

The major difference between the general reservoir rock sequence and that of the vein host rocks is the composition of the clay component. The normal reservoir sandstones are cemented by a mixture of illite and mixed-layer clays, with subordinate amounts of chlorite, while the authigenic clays in the vein hostrock are dominated by chlorite. Since the detrital mineralogy of both types of sandstone is similar and there is no reason to expect that the sandstones hosting the veins were buried to any greater depths than the other reservoir sandstones, the fluids from which the clays were precipitated must have differed. The precipitation and alteration of clay assemblages is largely controlled by the pore fluid chemistry, with illite-smectite associations resulting from solutions high in  $K^+$  ions, and chlorite assemblages result from fluids rich in  $Mg^{2+}$  ions. The proximity of the chlorite cements to the fractures may be related to Mg-rich fluids which migrated along these fractures. The significance of this is discussed below.

#### ANALYSIS OF GILSONITE

Two main varieties of gilsonite may be observed in the veins; generally referred to as massive and pencillate forms. Many veins exhibit a centre of massive gilsonite flanked on either wall by a zone of pencillate gilsonite. The 'pencils' are usually orientated sub-parallel with the vein wall and are generally horizontal to sub-horizontal. Some veins only exhibit one or the other variety. Massive gilsonite shows a conchoidal fracture, while the pencillate form fractures parallel to the pencillate fabric.

Reflected light, SEM, and electron probe investigations were performed on the gilsonite from the veins. The reflected light analysis showed the gilsonite to have uniformly low reflectances ranging from 0.2 - 0.3% $R_0$  indicating that the bitumen is thermally immature. No significant difference between the reflectance of the pencillate and massive forms of gilsonite were observed. Neither was any evidence for flow textures seen within the gilsonite.

Numerous small voids ranging in size from  $<1\mu\text{m}$  to in excess of 1 mm diameter were observed both in hand specimen and under the SEM (Fig. 14). SEM analysis also shows the pencillate texture to be the result of numerous parallel to sub-parallel fractures. However, there is no apparent displacement across the fractures, and they may be more properly classified as joints.

## FLUID INCLUSION ANALYSIS

Although no suitable material for fluid inclusion analysis was obtained from the gilsonite veins, authigenic quartz crystals up to 1.5 mm in length containing simple two phase fluid inclusions up to  $100\mu\text{m}$  (Fig. 15), were recovered from a wurtzilite vein (a similar solid hydrocarbon) in an abandoned mine at Indian Canyon 40 miles to the north west of the area. The quartz gave homogenization temperatures ranging from  $92\text{-}109^{\circ}\text{C}$  and an average of  $98^{\circ}\text{C}$ . These temperatures are generally regarded as those which are characteristic of the early stages of hydrocarbon generation (Hunt 1979), (Fig. 16).

## MODELS OF VEIN FORMATION

### Fracture development

The presence of other mineral coatings seen on the vein walls predating the gilsonite indicates that the fractures were present before the injection of the gilsonite. Therefore two processes were involved in the development of the veins; the formation of the original fracture and the subsequent injection and solidification of hydrocarbon.

Fractures may be classified into two broad sub-divisions, tensional and shear, and in investigating joint formation it is important to identify which type of fracture is involved. Shear fractures normally occur in conjugate arrays whereas tensional fractures generally occur as a single set perpendicular to the axis of the minimum principal stress. The lack of slip striae, preservation of plume structures, and development of a single set of fractures are consistent with a tensional origin for the fractures which were precursors to the gilsonite veins. These observations are consistent with the

observations of Narr and Currie (1982), who suggest that fractures formed in the Altamont oil field (Fig. 1) and more generally throughout the Uinta Basin are tensional rather than shear fractures.

A model for joint formation involves the hydrofracturing of the host rocks with the trend of the fractures being perpendicular to the local  $\sigma_3$  orientation. Fracture formation occurs when the pore fluid pressure, P, exceeds the minimum compressive stress,  $\sigma_3$ , plus the tensile strength of the rock T :

$$\sigma_3 - P \geq T$$

Deviations in the trend of the fractures are consistent with local variation in the  $\sigma_3$  orientation and also may have been influenced by underlying fault systems such as the Gar Mesa .

This mechanism requires high formation pressures within the fractured sequence. The production of large volumes of hydrocarbon from the Green River Formation and the very low permeability of this source rock allowed high pressures to develop, and it is feasible that the fracture developed to restore pressure equilibrium. The hydrofracturing occurred due to the build up of pressure below or within impervious strata, which prevented fluid expulsion, until the above equation was satisfied and the rock failed, producing a fracture (Price 1978). Any fluid accumulated below will then be injected upward, increasing the hydrostatic pressure in the overlying strata and extending the fractures into the upper parts of the succession system. Fracture growth only ceases when the hydrostatic pressure no longer exceeds the confining pressure plus the tensile strength of the rock.

The development of high formation pressures may be related to a number of processes including the entrapment of connate waters in the sediment pile, dewatering reactions occurring in clay-rich horizons as burial proceeds or the production of carbon dioxide prior to the generation of hydrocarbons. The Green River Formation is likely to

have experienced such high pressures before the main episode of hydrocarbon formation because:

- 1) The Green River Formation could act as an impervious layer.

- 2) The Green River Formation could contribute to elevated formation pressures due to dewatering reactions in the clay component and by the development of carbon dioxide prior to hydrocarbon generation. Fractures observed below this sequence could also develop at this stage because the high pore pressures developed below the Green River Formation would also favour the development of hydraulic fractures.

The above observations are further substantiated by the composition of the authigenic clay component of the host sandstones . Fluids produced from the Green River Formation would be expected to contain high concentrations of  $Mg^{2+}$  due to the dissolution of dolomite. This is consistent with precipitation of chlorite as the predominant clay mineral.

#### **Gilsonite Injection.**

The second phase of vein formation would have been the injection of hydrocarbons. The association of offshoots and impregnated sandstones with the gilsonite veins indicates that the hydrocarbon was injected under considerable pressure. It is likely that the injection of the gilsonite was the cause of the dilation seen in the veins. If the veins were injected with the minimum principal stress perpendicular to the basin axis, the apparent sinistral stepping seen in the veins could be explained by opening of the fractures normal to the minimum principal stress (i.e. N-S) rather than perpendicular to their trend (i.e. ENE-WSW). Dilation in this orientation would cause offsets in the fracture to open obliquely to the vein and thus produce an apparent sinistral displacement (Fig. 17).

High pressures may be linked with overpressuring developed as described above, and especially as a consequence of hydrocarbon generation. Subsequent solidification was probably caused by degassing associated with the release of pressure as the hydrocarbon migrated through the fractures. Degassing allows the release of volatile components

from the liquid hydrocarbons to leave a heavier residue prone to solidification (Rogers and others 1974). This solidification prevented the loss of the hydrocarbon and the closure of the fractures. SEM analysis of gilsonite reveals numerous small (up to 1mm) bubbles which once may have contained the escaping gasses, possibly methane and other light hydrocarbons, conforming with the observations of gas pockets adjacent to the veins by Crawford (1949). In a number of the veins the bubbles are seen to be elongate parallel to the vein walls, which may indicate a lateral as well as vertical migration of hydrocarbons through the veins, due to lateral flow extending the voids in the direction of movement. Reflectance techniques were used to investigate if flow textures were present within the gilsonite but no conclusive evidence was observed.

## ORIGIN OF GILSONITE

The most likely source for the hydrocarbon was the organic-rich Green River Formation. The maximum depth of burial of the Green River Formation in the eastern Uinta basin was probably no greater than 1500m, which allowing for slightly raised geothermal gradients, was not deep enough for the generation of light crude oil (Hunt 1979). This is confirmed by a burial reconstruction for the area using the Lopatin method (Waples 1980). Using formation thicknesses derived from borehole data (Crawford 1949), age data from Sweeny and others (1987) and assuming a geothermal gradient similar to that of the present day at  $25^{\circ}\text{C km}^{-1}$  with a surface temperature of  $20^{\circ}\text{C}$ , the base of the Green River Formation only reaches 2.8 TTI (Fig. 18). This is below the TTI value of 15 generally held as that required for the onset of hydrocarbon generation. However there is other overwhelming evidence that the Green River Formation was indeed the source of the gilsonite veins, and some associated oil:

(i) Some veins have such a limited vertical and lateral extent that they can be related directly to an oil-shale source, and small fractures within the shales are commonly filled with the gilsonite (Hunt 1963).

(ii) The majority of veins occur on the eastern side of the basin where the shales have high organic carbon contents and the thickness of good quality oil-shale is

greatest (Fig. 1). Gilsonite veins are lacking on the western side of the basin where the Green River Formation is not so carbonaceous. A number of WNW-ESE fractures in the Wasatch Formation further south are also devoid of gilsonite.

(iii) Gas chromatography of the gilsonites from different districts shows distinctions which can be related to variations in kerogen type between the central and peripheral parts of the Green River Formation palaeolacustrine system (Douglas and Grantham 1974).

(iv) Gas chromatography - mass spectrometry shows a correlation between extracts from the gilsonite and the Green River Formation oil-shales and also correlation between bitumen type (gilsonite, ozocerite) and the composition of oils which occur in the bitumen country rock (Hunt 1979) (Fig. 19).

(v) Infra-red spectra show a correlation between gilsonite and the Mahogany Ledge oil-shale of the Green River Formation (Hunt 1963).

(vi) A correlation between bitumens and stratigraphic level is evident from sulphur isotopic compositions, and suggests that the organically-bound sulphur originates from the lacustrine host sediments (Harrison and Thode 1958, Mauger and others 1973).

Hydrocarbons generated at such a shallow burial depth from immature oil-shales would be expected to have an immature character. Accordingly oil in the Green River Formation in the eastern Uinta Basin is found to be immature (Anders and Gerrild 1984) and the gilsonite is highly aromatic, also typical of immature oils (Hunt 1979). It is notable that in the case of the Green River Formation oil shales either the Lopatin model cannot be applied or, more probably, the stratigraphic or geothermal evidence for the area is incorrect and some other factors may need to be taken into account. The fact that the fluid inclusion results from other parts of the basin are in excess of the predicted temperatures would tend to support this. However, since the hydrocarbons exhibit an immature nature this suggests that they would be produced before the onset of the oil window as proposed by Lopatin. The Black Dragon Vein extends stratigraphically downward into the Wasatch Formation. It seems improbable that this vein has a different source from the numerous other veins in the area. If a high

pressure zone related to the Green River Formation had developed it would be feasible for the hydrocarbon to migrate both upward and downward away from the higher pressure zone associated with hydrocarbon generation. High pressures are indicated from the small lateral offshoots which have been injected along bedding in finely laminated sediments at a number of localities. The presence of two fractures at Black Dragon which exhibit gilsonite impregnation within the wall rock without the development of a gilsonite vein may be related to higher confining pressures developed in the Wasatch compared to overlying formations.

#### TIMING OF VEIN FORMATION

The exact timing of the fracturing and gilsonite events is difficult to ascertain although it is obvious from the discussion above that the two events must be separated by some period of time. It is probable that hydrocarbon generation from the Green River Formation kerogen occurred while the succession was at its maximum burial depth (30-10 Ma) and thus vein formation occurred during this period but this inference must be treated with caution.

#### SIGNIFICANCE OF EXPULSION RATE

The close correlation between the distribution of gilsonite veins and the greater thickness of high grade Green River Formation oil shale (yield > 15 gal/ton oil shale, data from Cashion 1967) shown in Figure 1 is particularly good evidence for the source of gilsonite in the Green River Formation. The oil shales are known to be a hydrocarbon source rock of very high potential in terms of both quantity and quality. The kerogen in the oil shales is type I (algal) kerogen (Tissot and others 1978) and accordingly has a high oil yield expressed as a hydrogen index up to 1000 mg/g. Similar very high values are also found in some other sequences which host prominent bitumen veins, including the Carboniferous Albert Formation of New Brunswick and the Permian of the Junggar Basin, North West China (Fig. 20). Each of these sequences is within a continental basin, including lacustrine (algal) source rocks, which experienced rapid burial beneath

siliciclastic sediments. We believe that the shared characteristics of exceptional yield and rapid burial are significant. Together these factors suggest that once hydrocarbon generation had commenced at a significant rate, enormous volumes of hydrocarbon would be generated within a short period of time. The normal pathways for fluid migration from source rocks (interparticulate or microfractures) may be inadequate to cope with such large volumes, and rapidly cause the development of overpressuring as described above. The source rocks would effectively become saturated with hydrocarbon at an early stage of thermal maturation and oil would be expelled as a separate phase.

The possibility of inducing fracturing in source rocks during oil generation has been suggested by numerous workers (Momper 1978, du Rouchet 1981, Mann 1990, Lucas and Drexler 1976). At very high rates of oil generation the pore network in the mudrocks would be inadequate for the rapid expulsion needed, and the pore pressure would exceed the mechanical strength of the rocks and result in fracturing. Further discussion of the mechanisms of fracturing in low permeability source rocks is given by Ozkaya (1988).

The release of excess pressure by fluid escape into a major fracture system would explain the large volumes of relatively pure bitumen in the fractures. In the Green River Formation oil expulsion occurred before the main phase of oil generation had been achieved. Oil saturation may occur at a very early stage in prolific source rocks, and a similar generation of oil into fractures early during thermal maturation has been documented in the Woodford Formation of Arkansas and Oklahoma (Comer and Hinch 1987).

## CONCLUSIONS

The gilsonite veins were formed in at least two separate phases. A joint set developed, possibly as a result of hydrofracturing related to abnormal formation pressures. Subsequently hydrocarbons were injected into the fractures to produce the gilsonite veins, in a N-S oriented stress field. The gilsonite was sourced in the Green River Formation and overpressuring developed as a result of the generation of

substantial volumes of hydrocarbons. This model can be applied to a number of similar occurrences throughout the world.

#### ACKNOWLEDGEMENTS

We acknowledge with pleasure the help given during field studies by the staff of the American Gilsonite Company, the Zeigler Company and the Lekas Mining Company. The support of the Utah Geological and Mineralogical Survey and technical help from E. Mulqueeney, M. Pringle and the Staff of the Queen's University Electron Microscope Unit. BM is in receipt of a postgraduate studentship from the Department of Education (Northern Ireland).

#### REFERENCES

ANDERS, D.E. and GERRILD, P.M., 1984, Hydrocarbon generation in lacustrine rocks of Tertiary age, Uinta Basin, Utah, organic carbon, pyrolysis yield and light hydrocarbons: *in*, WOODWARD, J., MEISSNER, F.F., and CLAYTON, J.L., Hydrocarbon source rocks of the greater Rocky Mountains: Rocky Mt. Ass. of Geologists.

CASHION, W.B., 1967, Geology and fuel resources of the Green River Formation, southeastern Uinta Basin, Utah and Colorado: U.S. Geologists Survey Professional Paper, 548, 48pp.

COMER, J.B., and HINCH, H.H., 1987, Recognizing and quantifying expulsion of oil from the Woodford Formation and age-equivalent rocks in Oklahoma and Arkansas: American Association of Petroleum Geologists Bulletin. v.71, 844-858.

CRAWFORD, A.L., 1949, Gilsonite and related hydrocarbons of the Uinta Basin, Utah: Utah Geol. and Mineralog. Survey Oil and Gas Possibilities of Utah, p. 235-260.

DOUGLAS, A.S., and GRANTHAM, 1974, Fingerprint gas chromatography in the analysis of some native bitumens, asphalts and related substances: *in* TISSOT, B., AND BIENNER F., Advances in organic geochemistry. 1973 (Editions Techup, Pass), p. 261-276.

ELDRIDGE, G.H., 1896, The Uintaite deposits of Utah: U.S. Geological Survey 17<sup>th</sup> Ann. Rep. Pt.1, p. 909-949.

HARRISON, A.G., and THODE, H.G., 1958, Sulphur isotope abundances in hydrocarbons and source rocks of the Uinta Basin, Utah: American Association of Petroleum Geologists Bulletin. v42, p2642-2649.

HUNT, J.M., 1963, Composition and Origin of the Uinta Basin Bitumens: Utah Geol. and Minerolog. Surv. Bull. v.54, p249-273.

HUNT, J.M., 1979, Petroleum geochemistry and geology: Freeman's San Francisco. 617pp.

LOPATIN, N.V., 1971, Temperature and geological time as factors in coalification (in Russian). Izv. Akad. Nauk SSSR, Seriya geologicheskaya, No. 3, p95-106.

LUCAS, P.T., and Drexler J.M., 1976, Altamont-Bluebell - a major naturally fractured stratigraphic trap, American Association of Petroleum Geologists Memoir 24, North American Oil and Gas Fields, p. 121-135.

MANN, U., 1990, Sedimentological and petrophysical aspects of primary petroleum migration pathways: In HELING, D., ROTHE, P., FORSTNER, U., and STOFFERS, P., (eds) Sediments and environmental geochemistry. Springer-Verlag, Berlin, p152-178.

MAUGER, R.L., KAYSER, R.B., and GWYNN, J.W., 1973, A Sulphur isotopic study of Uinta Basin hydrocarbons: Utah Geological and Mineralogical Survey Special Studies 41.

MOMPER, J.A., 1978, Oil migration limitations suggested by geological and geochemical considerations: In Roberts, W.H., and Cordell R., (eds) Physical and chemical constraints on petroleum migration. American Association of Petroleum Geologists Course Note 8, B1-B60.

NARR, W., and CURRIE, J.B., 1982, Origin of fracture porosity-example from Altamont Field, Utah: American Association of Petroleum Geologists Bulletin. v.66, p1231-1247.

OZKAYA, J., 1988, A simple analysis of oil induced fracturing in sedimentary rocks: Mar. Petrol. Geol. v.5, 293pp.

PITMAN, J.K., FOUCH, T.D., AND GOLDHABER, M.B., 1982, Depositional setting and diagenetic evolution of some Tertiary unconventional reservoir rocks, Uinta Basin, Utah: American Association of Petroleum Geologists Bulletin. v.66, p1581-1596.

PRICE, N.J., 1978, Fault and joint development in brittle and semi-brittle rock: Pergamon, Oxford.

PRUITT, R.G., 1961, The mineral resources of Uinta County, Utah: Utah Geological and Mineralogical Survey Bulletin v.71, pp101.

ROGERS, M.A., M<sup>C</sup>ALARY, J.D., and BAILEY, N.J.L., 1974, Significance of reservoir bitumens to thermal maturity studies, Western Canada Basin: American Association of Petroleum Geologists Bulletin. v.58, p1806-1824.

ROUCHET, J. DU, 1981, Stress fields, a key to oil migration: American Association of Petroleum Geologists Bulletin. v.65, p63-73.

SPENCER, C.W., 1987, Hydrocarbon generation as a mechanism for overpressuring in Rocky Mountain region: American Association of Petroleum Geologists Bulletin. v.71, p368-388.

SWEENEY, J.J., BURNHAM, A.K. and BRAUN, R.L., 1987 A model for hydrocarbon generation from type I kerogen: Application to the Uinta Basin, Utah: American Association of Petroleum Geologists Bulletin. v.71, p967-985

TISSOT, B., DERRO, G., and HOOD, A., 1979, Geochemical study of the Uinta Basin: Formation of petroleum from the Green River Formation: Geochem et Cosmochem Acta v.42, p1469-1485

WAPLES, D., 1980. Organic geochemistry for exploration geologists. Burgess Publishing Company, Minneapolis. p95-106

## FIGURE CAPTIONS

Fig. 1. Location map of Uinta Basin, Utah showing main oil fields and isopachts for the Green River Oil Shale (Yield > 15 gal/ton oil shale, data from Cashion 1967). Note the correlation between oil shale thickness and vein distribution.

Fig. 2. Stratigraphic and related vein morphology for the eastern Uinta Basin. (Wall mine)

Fig. 3. Spatial block rose digram ( $10 \text{ km}^2$ ) showing the deviations in the overall trend of the gilsonite veins. (B = Bonanza, O = Ouray and FD = Fort Duchene.)

Fig. 4. Diagram indicating major features of gilsonite vein morphology.

Fig. 5. Micrograph of authigenic quartz crystals nucleated on breccia within gilsonite. (Field width, 3mm).

Fig. 6. Composite diagenetic sequence for host sandstones.

Fig. 7. Margin of gilsonite vein showing gilsonite impregnation of patchily-cemented sandstone wallrock and grains floating in gilsonite vein proper, EB vein, (Field width 3mm)

Fig. 8. Sand grains exhibiting overgrowth, within gilsonite, Dragon Vein. Rough surface of gilsonite due to weathering. (Field width  $300\mu$ )

Fig. 9. Gilsonite veinlets extending into sandstone from which grains are partially detached, EB vein. (Field width 1mm)

Fig. 10. Mudrock clast within gilsonite exhibiting fracture and displacement by gilsonite, Independent vein (Field width 3mm)

Fig. 11. Bitumen veinlet extending from kerogen laminae, Green River Formation oil shale, base of Tabor vein. (Field width  $500\mu$ ).

Fig. 12. Dolomite crystals (bright) in gilsonite, Dragon vein, Black Virgin Mine. Cracking of gilsonite due to weathering. (Field width  $500\mu$ ).

Fig. 13. Calcite spherules (hollow) within gilsonite, base of Tabor vein, (Field width 2mm).

Fig. 14. Highly vesicular gilsonite, Harrison vein. Note elongate nature of vesicles. (Field width  $500\mu$ ).

Fig. 15. Authigenic quartz crystals in wurtzillite, Indian Canyon. Note cavity probably due to exhumed fluid inclusion in quartz. (Field width 1mm).

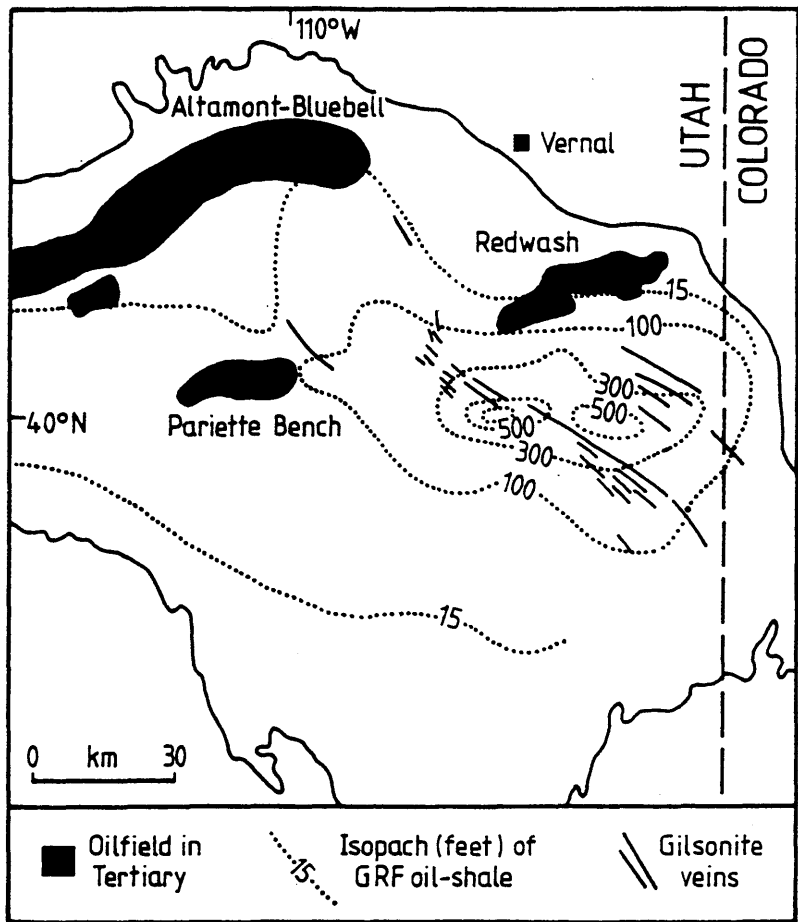
Fig. 16. Histogram of results of fluid inclusion analysis of material from wurtzillite from Indian Canyon.

Fig. 17. Mechanism of oblique dilation of fractures yielding apparent sinistral displacement seen on gilsonite veins.

Fig. 18. Burial reconstruction and Lopatin analysis for vein host rocks indicating low TTI (Time-Temperature Index, after Lopatin 1971) results suggesting that the Green River Formation is thermally immature. Note however the rapid burial rates indicated from the reconstruction.

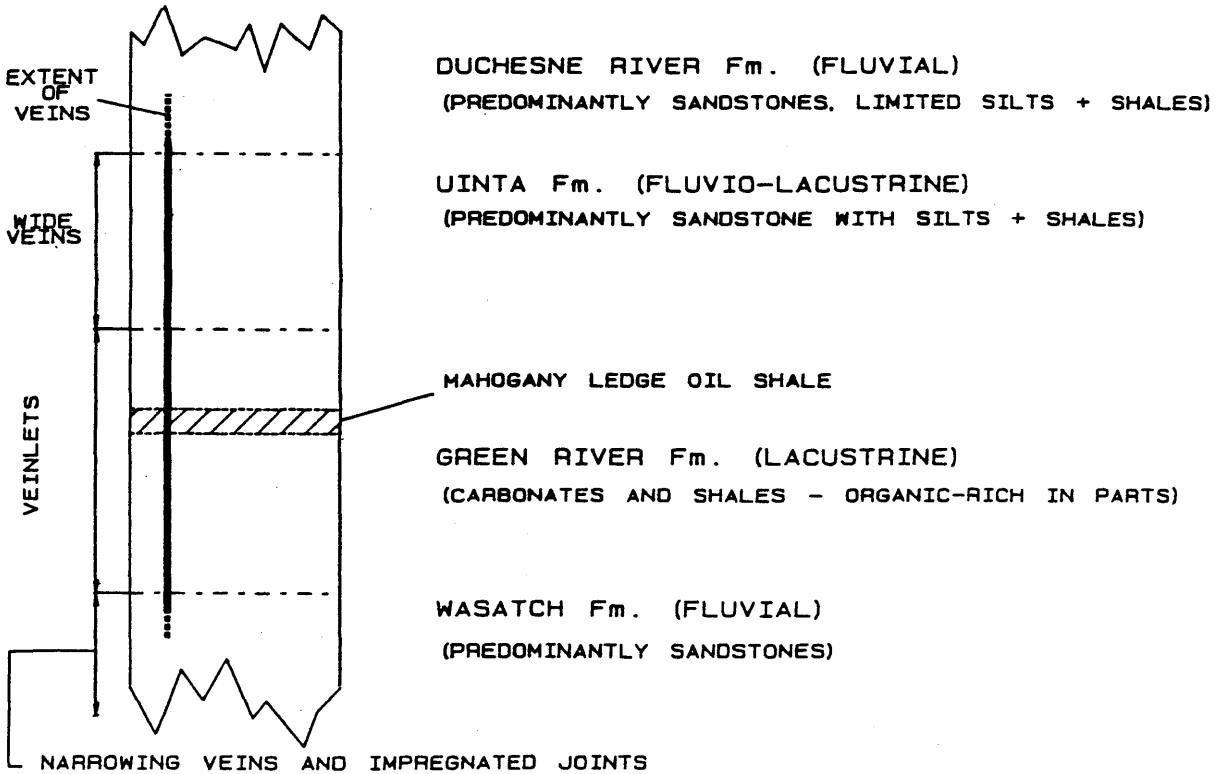
Fig 19. Composition of bitumens and oils from the Duchene oil field ( data from Hunt 1979 ). Gilsonite and 914m oil from the Green River Formation, ozocerite and 2315m oil from the Wasatch Formation.

Fig. 20. Van Krevelin Diagram showing kerogen type for three basins containing well developed bitumen veins.

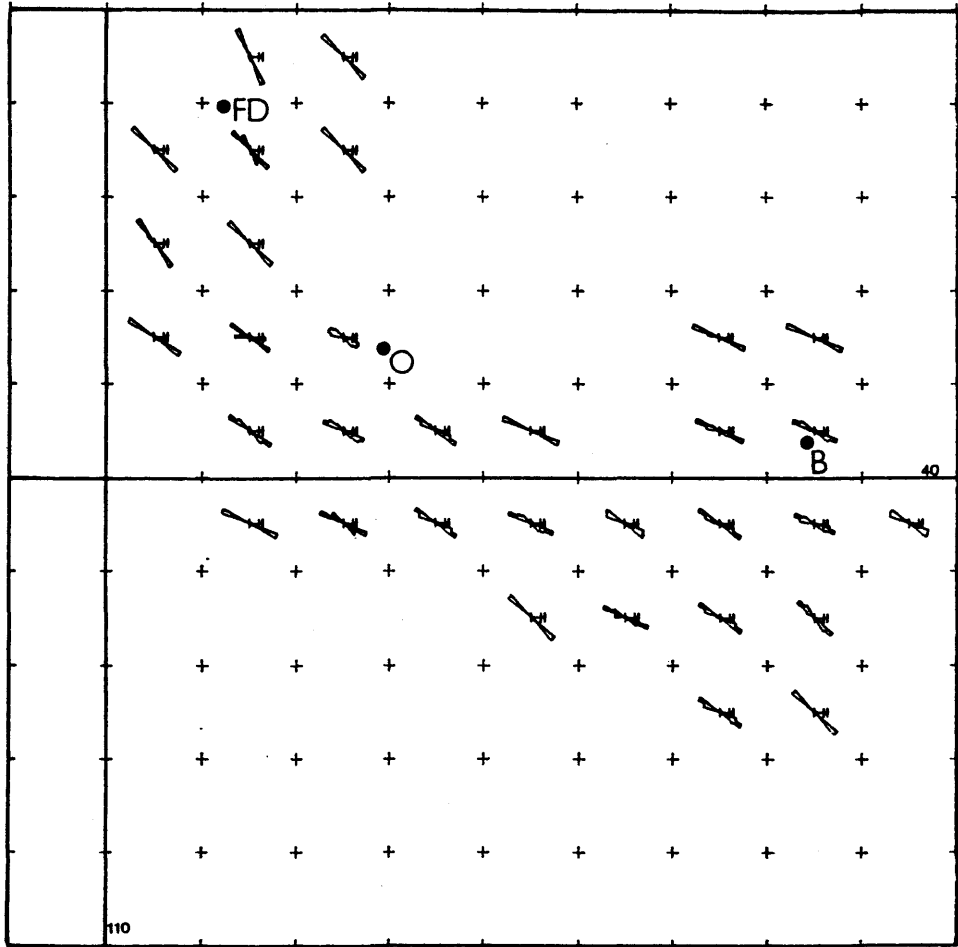


2

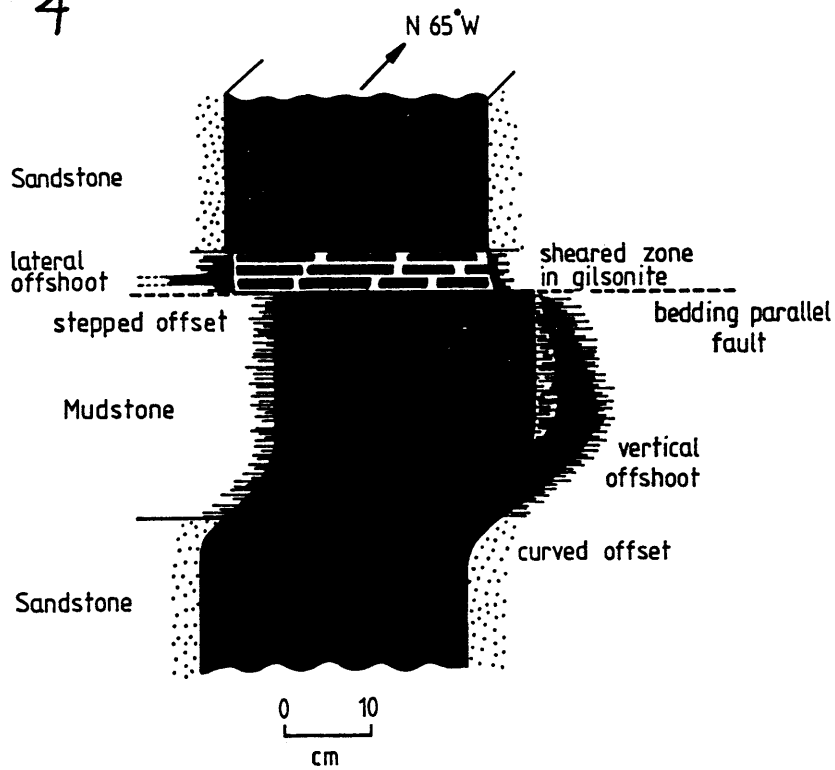
STRATIGRAPHY AND VEIN MORPHOLOGY, EASTERN UINTA BASIN, UTAH.



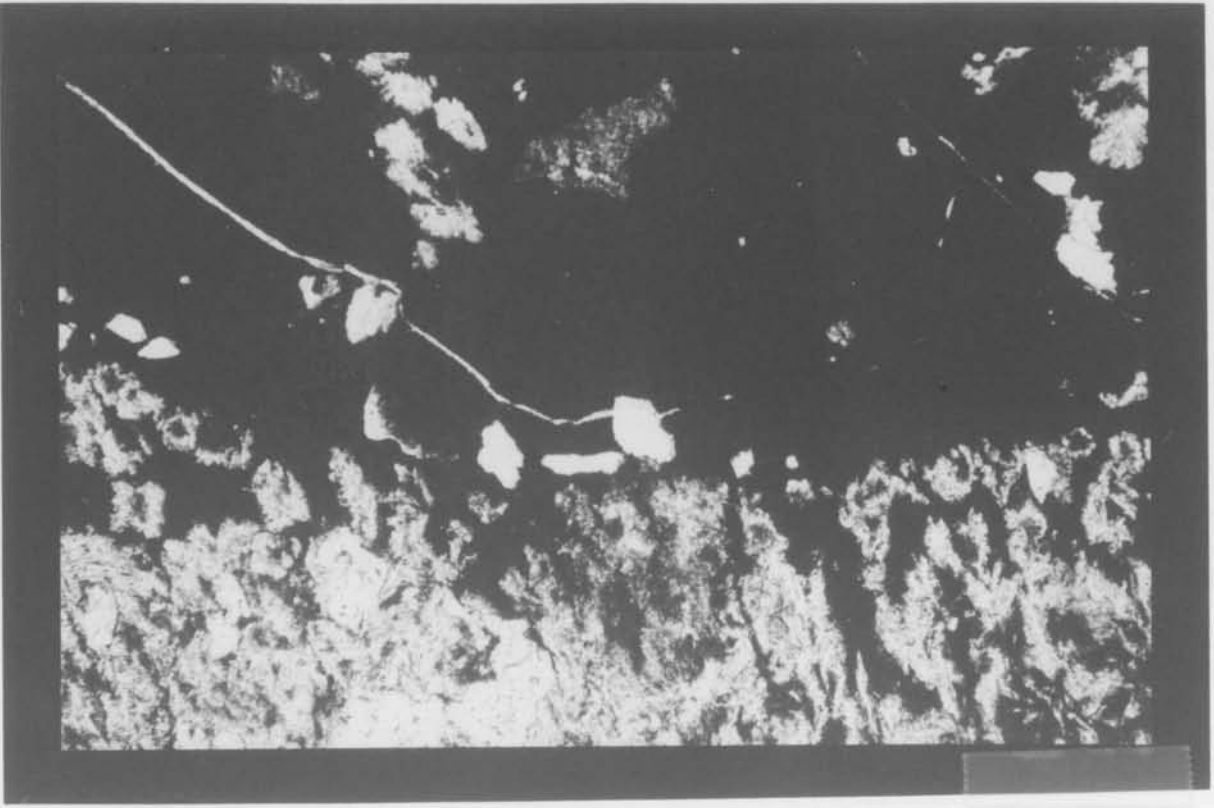
3



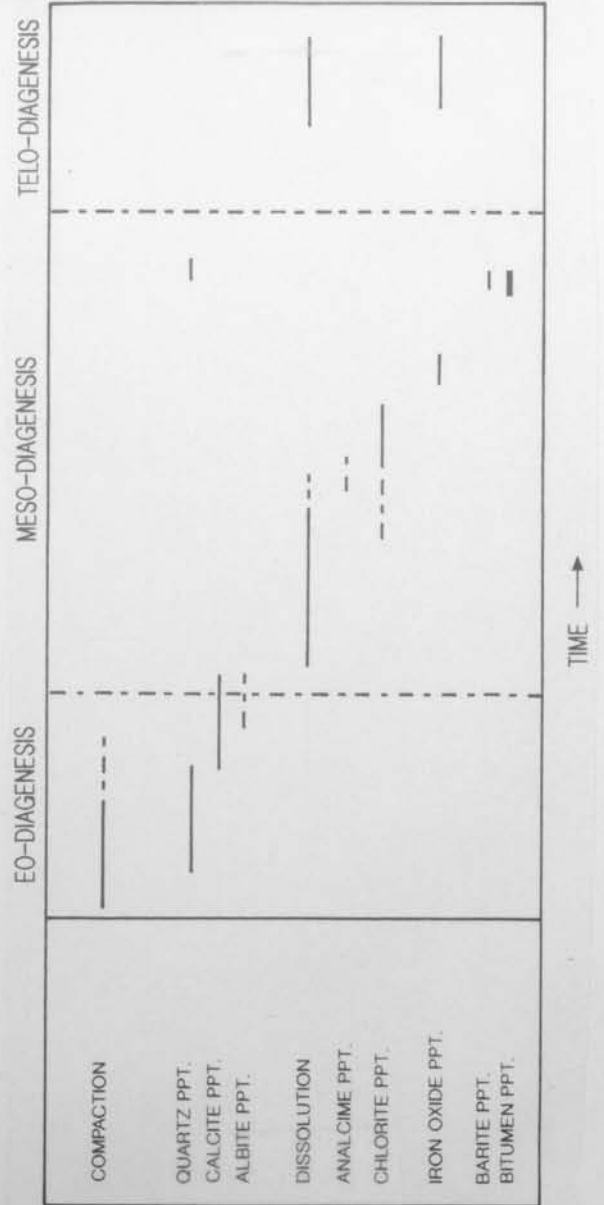
4



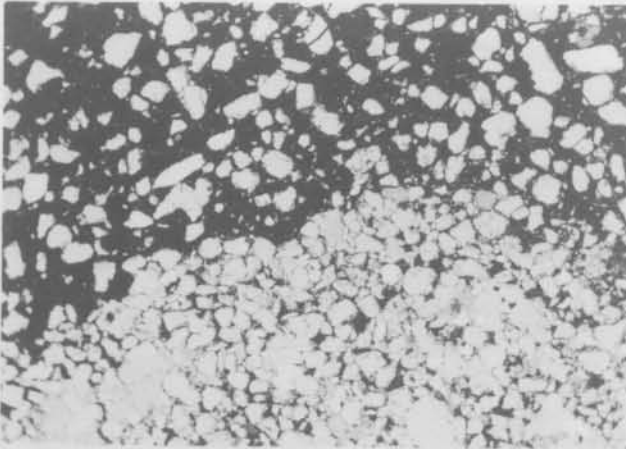
5



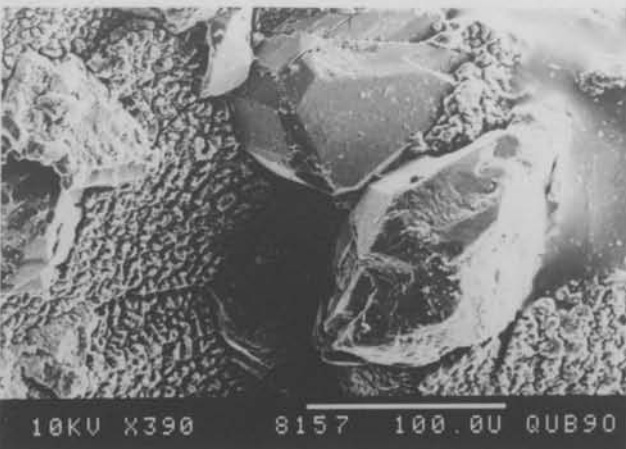
6



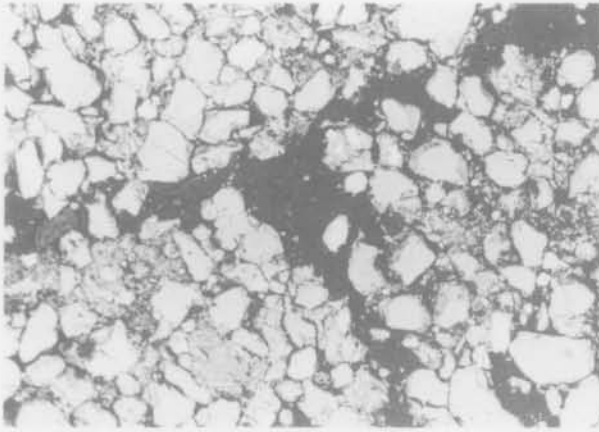
7



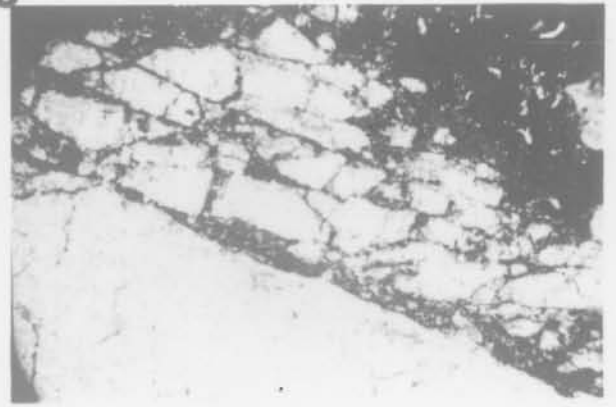
8



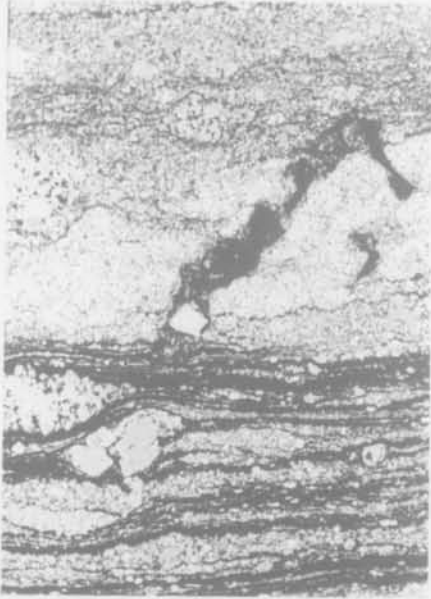
9



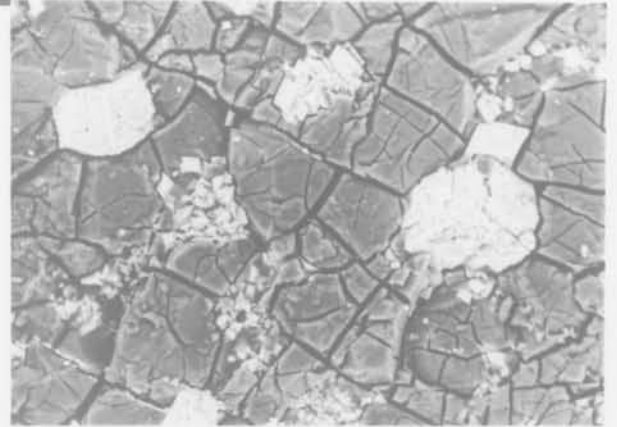
10



11



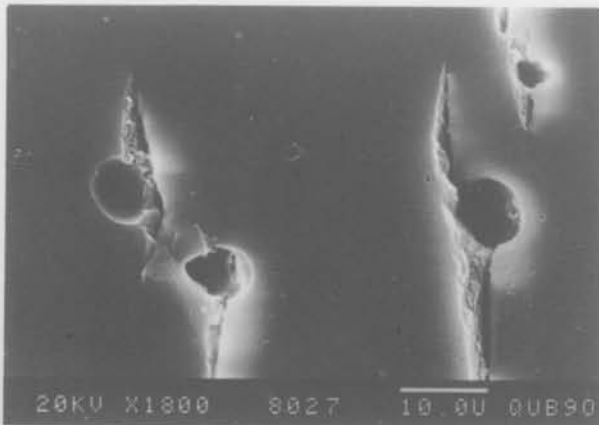
12



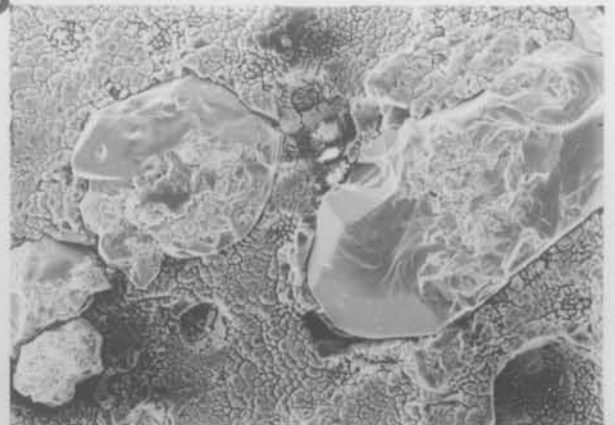
13



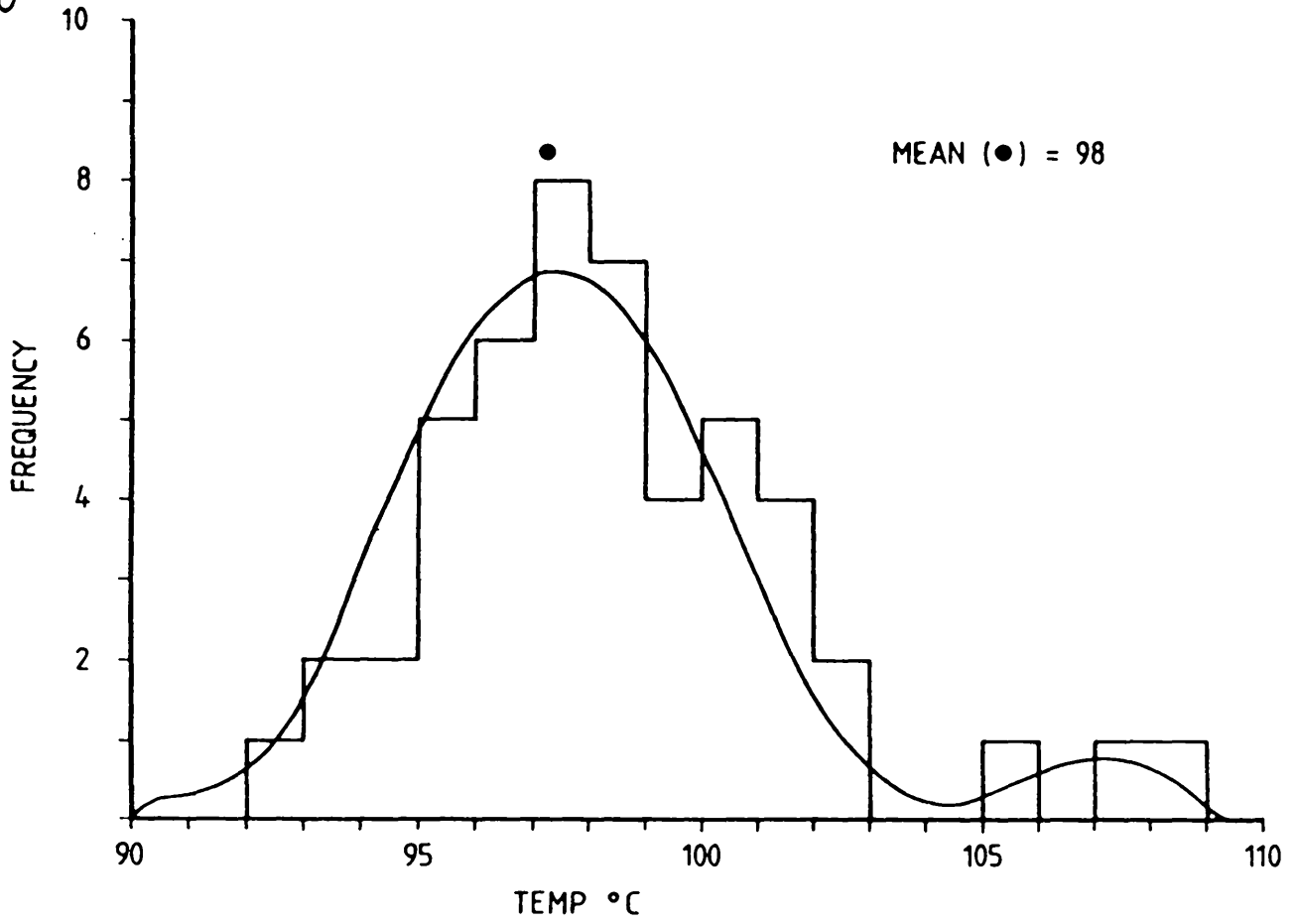
14



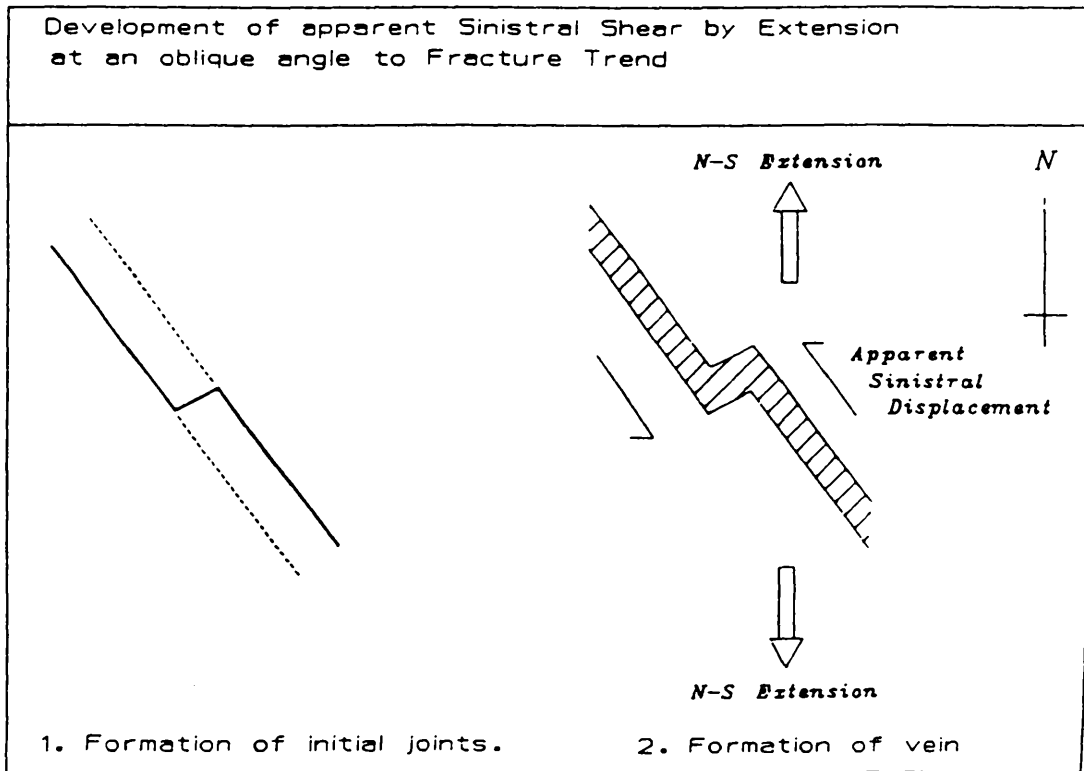
15



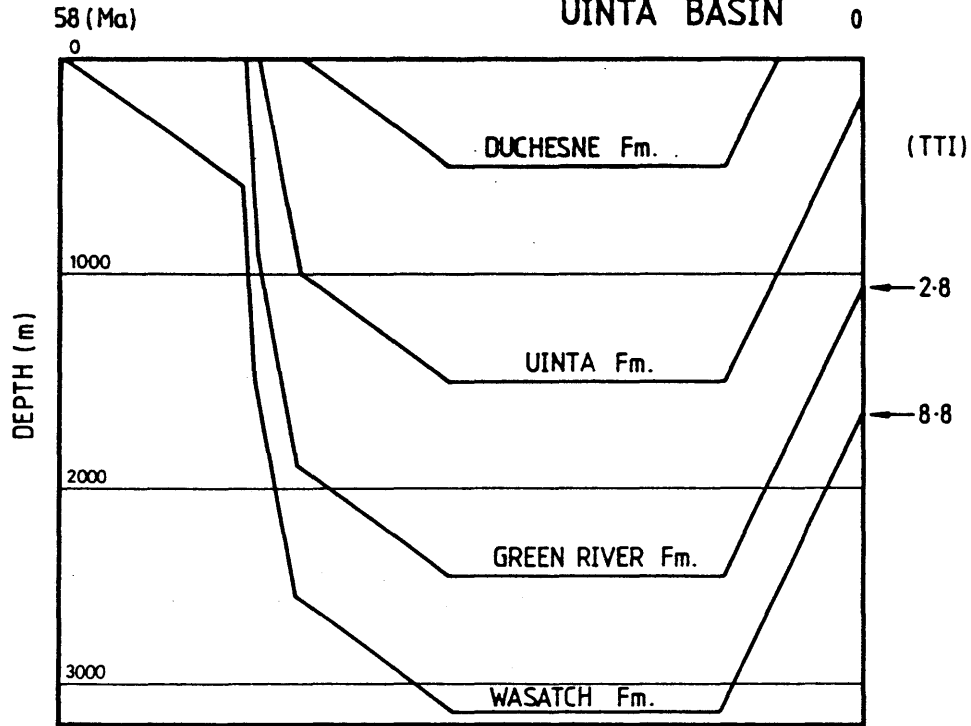
16



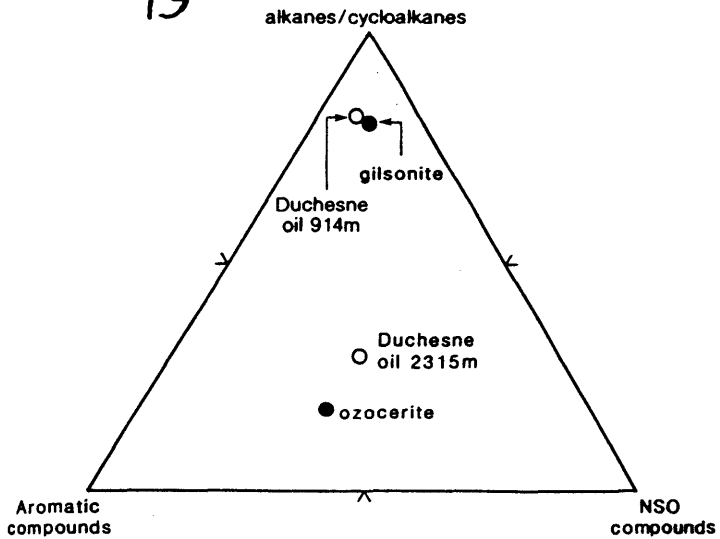
17



# 18 LOPATIN RECONSTRUCTION FOR THE EASTERN UINTA BASIN



19



20

